Journal of Alzheimer's Disease 101 (2024) 159–173
DOI 10.3233/JAD-240523
IOS Press

A Predictive Model of the Progression to Alzheimer's Disease in Patients with Mild Cognitive Impairment Based on the MRI Enlarged Perivascular Spaces

Jun Chen, Jingwen Yang, Dayong Shen, Xi Wang, Zihao Lin, Hao Chen, Guiyun Cui, Zuohui Zhang* and the Alzheimer's Disease Neuroimaging Initiative[1]
Department of Neurology, The Affiliated Hospital of Xuzhou Medical University, Xuzhou, China

Accepted 13 June 2024
Pre-press 22 August 2024

Abstract.
Background: Mild cognitive impairment (MCI) is a heterogeneous condition that can precede various forms of dementia, including Alzheimer's disease (AD). Identifying MCI subjects who are at high risk of progressing to AD is of major clinical relevance. Enlarged perivascular spaces (EPVS) on MRI are linked to cognitive decline, but their predictive value for MCI to AD progression is unclear.
Objective: This study aims to assess the predictive value of EPVS for MCI to AD progression and develop a predictive model combining EPVS grading with clinical and laboratory data to estimate conversion risk.
Methods: We analyzed 358 patients with MCI from the ADNI database, consisting of 177 MCI-AD converters and 181 non-converters. The data collected included demographic information, imaging data (including perivascular spaces grade), clinical assessments, and laboratory test results. Variable selection was conducted using the Least Absolute Shrinkage and Selection Operator (LASSO) method, followed by logistic regression to develop predictive model.
Results: In the univariate logistic regression analysis, both moderate (OR = 5.54, 95% CI [3.04–10.18]) and severe (OR = 25.04, 95% CI [10.07–62.23]) enlargements of the centrum semiovale perivascular space (CSO-PVS) were found to be strong predictors of disease progression. LASSO analyses yielded 12 variables, refined to six in the final model: APOE4 genotype, ADAS11 score, CSO-PVS grade, and volumes of entorhinal, fusiform, and midtemporal regions, with an AUC of 0.956 in the training and 0.912 in the validation cohort.
Conclusions: Our predictive model, emphasizing EPVS assessment, provides clinicians with a practical tool for early detection and management of AD risk in MCI patients.

Keywords: Alzheimer's disease, mild cognitive impairment, nomogram, perivascular space

*Correspondence to: Zuohui Zhang, Department of Neurology, The Affiliated Hospital of Xuzhou Medical University, Xuzhou, 221006, China. E-mail: zuohuizhang@xzhmu.edu.cn.

[1]Data used in preparation of this article were obtained from the Alzheimer's Disease Neuroimaging Initiative (ADNI) database (http://adni.loni.usc.edu). As such, the investigators within the ADNI contributed to the design and implementation of ADNI and/or provided data but did not participate in analysis or writing of this report. A complete listing of ADNI investigators can be found at: http://adni.loni.usc.edu/wp-content/uploads/how_to_apply/ADNI_Acknowledgement_List.pdf.

INTRODUCTION

Alzheimer's disease (AD) is a complex neurodegenerative disorder that poses a significant healthcare challenge globally.[1] It is considered one of the most significant forms of dementia, affecting a cumulative total of 40 million individuals worldwide. This disease imposes significant suffering and burden on both patients and their families. Moreover, as the population ages, the number of individuals affected by AD continues to increase.[2] Mild cognitive impairment (MCI)is characterized by cognitive dysfunction in an individual beyond what is expected given their age or education. MCI is a heterogeneous condition that can manifest as cognitive impairment preceding various dementias. While MCI is not solely a precursor to AD, it is important to note that a significant proportion of individuals with MCI may progress to AD. Additionally, many individuals diagnosed with AD initially present with symptoms of MCI.[3] Therefore, it is important to identify individuals within the MCI cohort who are at a heightened risk of progression, enabling early detection and intervention.

Currently, established biomarkers like biochemical alterations in cerebrospinal fluid (CSF) and neuroimaging assessments of brain structure and function are validated as dependable indicators for AD.[4–6] These include elevated amyloid-β (Aβ) and tau protein levels in CSF, shrinkage of the hippocampus, and decreased activity in the posterior cingulate cortex. Machine learning algorithms that amalgamate these biomarkers have proven to enable highly accurate, automated diagnosis and prognosis in AD patients.[7,8] Nevertheless, due to variations in treatment standards and equipment across different regions, obtaining these biomarkers, such as PET-CT, is more challenging. Therefore, there is a need to discover biomarkers that are more accessible to clinical or community settings.

The perivascular space (PVS) acts as a conduit between neurovascular units and larger blood vessels, situated at the interface of small blood vessels and neurons, serving as a pathway for clearing metabolites, such as Aβ.[9] Normally, the perivascular space is not visible on magnetic resonance imaging (MRI). However, when there is increased CSF retention in the perivascular space due to various reasons such as degeneration or inflammation, the PVS expands and becomes visible on MRI.[10,11] Although previous studies generally concluded that enlarged perivascular space (EPVS) is not of significant importance, recent evidence suggests that the extent of EPVS visible on MRI can serve as an imaging marker for dysfunction in metabolite clearance.[12,13] An increased load of centrum semiovale perivascular space (CSO-PVS) has been associated with a higher risk of dementia, regardless of vascular risk factors, white matter hyperintensity, and recent small subcortical infarct.[14,15] This finding underscores the role of PVS as a subclinical MRI marker. Consequently, we attempted to explore the correlation between the severity of enlarged perivascular spaces in patients with MCI and the progression to MCI-AD through group analysis of different outcomes. Furthermore, we integrated EPVS load with clinical cognitive scales, biochemical markers, and other imaging features to devise a novel prediction model for assessing the risk of MCI-AD progression. This model aims to facilitate more convenient and accurate clinical screening of high-risk populations transitioning into dementia.

MATERIALS AND METHODS

ADNI study design

All study participants were drawn from the Alzheimer's Disease Neuroimaging Initiative (ADNI) database, including ADNI-1, ADNI-GO, ADNI-2, and ADNI-3 (https://adni.loni.usc.edu). Launched in 2003 as a collaborative effort between public and private sectors, ADNI aims to assess the feasibility of integrating serial MRI, positron emission tomography, biomarkers, clinical evaluations, and neuropsychological tests to measure the progression of MCI and early-stage AD. For the latest updates, refer to https://www.adni-info.org. Institutional review boards at all participating institutions granted approval for ADNI, and written informed consent was obtained from all participants at each site.

Participants

This study's cohort was selected from the vast array of demographic and clinical profiles available within the ADNI database. Our focused analysis included patients who were clinically diagnosed with MCI at baseline. These individuals underwent a comprehensive battery of assessments at the outset, encompassing MRI, blood tests, CSF analysis, and clinical evaluations, followed by periodic reviews extending from 3 to 36 months.

In the diagnostic criteria of the ADNI database, MCI is diagnosed based on memory complaints verified by a study partner, abnormal memory function documented by scoring below education-adjusted cutoffs on the Logical Memory II subscale, a Mini-Mental State Exam (MMSE) score between 24 and 30, Clinical Dementia Rating (CDR) of 0.5, and preserved general cognition and functional performance. AD diagnosis includes memory complaints, abnormal memory function, MMSE score between 20 and 26, CDR of 0.5 or 1.0, and meeting National Institute of Neurological and Communicative Disorders and Stroke, as well as the Alzheimer's Disease and Related Disorders Association (NINCDS/ADRDA) criteria for probable AD.

In our initial selection, we identified 400 individuals with MCI. Upon closer scrutiny, we excluded those with incomplete datasets or anomalies in image processing. This filtration yielded a refined sample of 358 subjects. Of these, 181 maintained their MCI status without progressing to AD (MCI-nonconverted, MCI-NC), while 177 experienced a progression to AD (MCI-converted, MCI-C) within the follow-up period. The AD diagnosis was anchored to the criteria established by the NINCDS/ADRDA.

For the purposes of analytical rigor, the remaining MCI participants were stratified into two distinct groups: a training cohort and a validation cohort, following an 85 : 15 split (comprising 303 and 54 patients). The schematic of our study's design, encapsulating the selection and division process, is depicted in Fig. 1.

Patient information

Clinical data and laboratory test results were retrieved from the ADNI website. Demographic information encompassed age, sex, and medical history regarding hypertension, diabetes, hyperlipidemia, and hypercholesterolemia. Baseline cognitive function was assessed using four neuropsychological scales: the Alzheimer's Disease Assessment Scale (ADAS) 13 and 11 Cognitive Subscale, the CDR, and the MMSE. Laboratory features included CSF levels of Aβ, phosphorylated tau protein (p-tau), total tau protein (t-tau), and the presence of the APOE ε4 genotype. Measurements of CSF $A\beta_{1-42}$ and tau levels were performed with the Elecsys® β-amyloid (1–42) CSF and the Elecsys® Tau CSF immunoassays on a cobas e 601 instrument.[16] APOE4 genotypes were obtained from DNA extracted from blood.[17] The data is also available in the 'UPENNBIOMK9.csv' file in the ADNI database. The volumes of the hippocampus, entorhinal cortex (Entorhinal), fusiform gyrus (Fusiform), middle temporal lobe (MidTemp), whole brain, and intracranial volume (ICV) were obtained from the ADNIMERGE dataset, a part of the ADNI database. The MRI images were processed at the Center for Imaging of Neurodegenerative Diseases at UCSF, cortical reconstruction and volumetric segmentation is performed with the FreeSurfer image analysis suite. The specific image processing procedures have been detailed in previous studies.[18,19] and can also be found in the ADNI methods section accessible at http://adni.loni.usc.edu/. A comprehensive summary of clinical variables and laboratory features is provided in Table 1.

PVS ratings

All patients underwent head MRI at either 1.5T or 3.0T, as part of the imaging protocol established by the ADNI.[20] The visual rating of enlarged perivascular spaces was performed by two neurologists, Chen Jun and Yang Jingwen, following the Edinburgh group regarding EPVS rating guidelines.[21] EPVS larger than 1 mm in diameter in the centrum semiovale (CSO) and basal ganglia (BG) were visually evaluated using MPRAGE and FLAIR images.The assessment of EPVS in CSO and BG was focused on the slices with the highest number of EPVS, graded based on the following scores: level 0 denoted no EPVS, level 1 indicated 1 to 10 EPVS, level 2 indicated 11 to 20 EPVS, level 3 indicated 21 to 40 EPVS, and level 4 indicated more than 40 EPVS, in accordance with established protocols.To aid statistical analysis, the EPVS data were categorized using various grading methods. For EPVS in CSO and BG, categories 0 and 1 were combined and labeled as no/mild (score = 1), category 2 was labeled as moderate severity (score = 2), and levels 3 and 4 were labeled as severe (score = 3).

Data analysis and model building

Continuous variables were summarized using median values, while categorical variables were described using proportions. Comparisons between MCI-C and MCI-NC were made using appropriate statistical tests tailored to the data type: Wilcoxon rank-sum test or *t*-test for continuous data, and Fisher's exact test or Pearson's Chi-square test for categorical data. To assess the predictive value of fac-

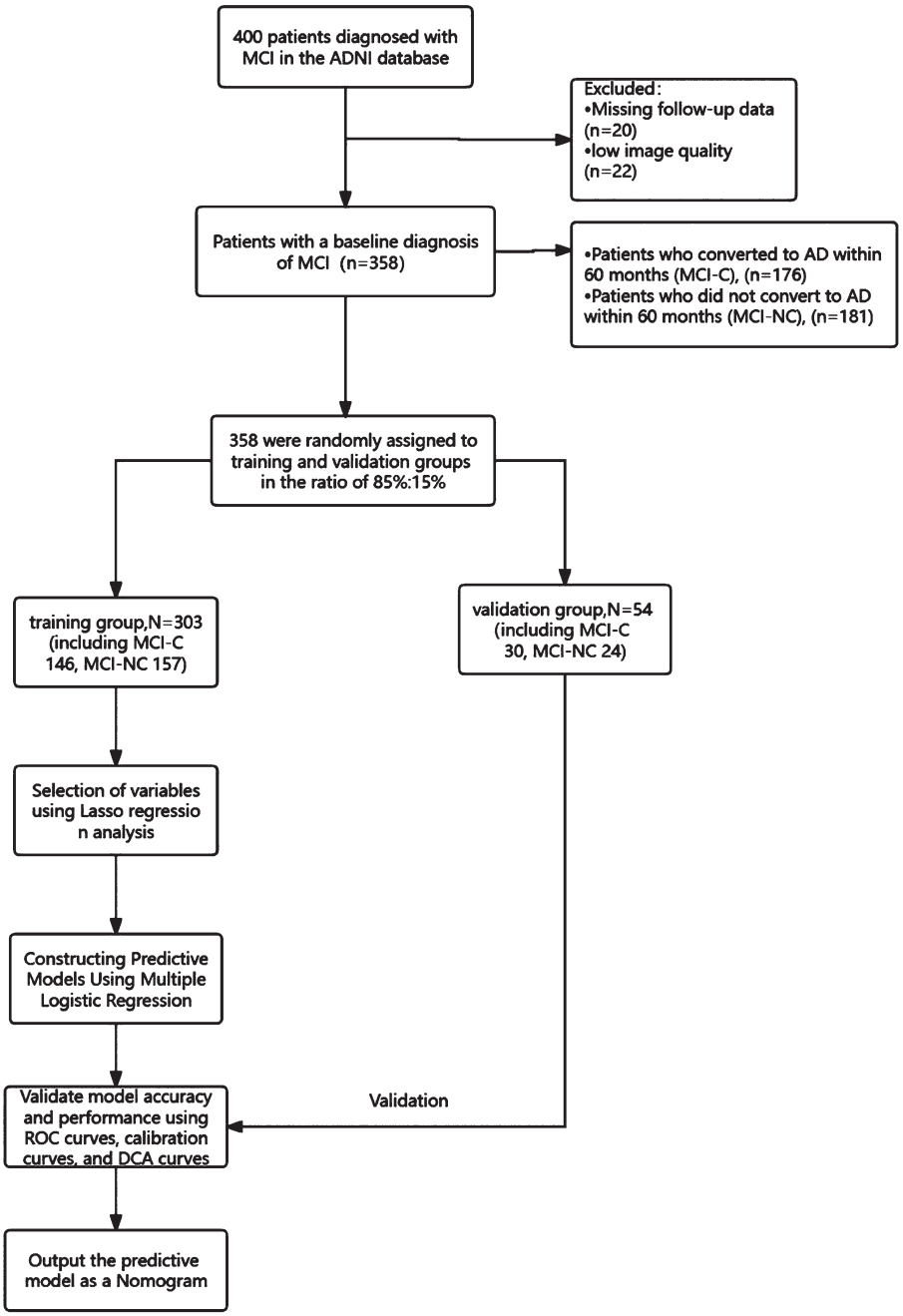

Fig. 1. MCI, mild cognitive impairment; ADNI, Alzheimer's Disease Neuroimaging Initiative; ROC, receiver operating characteristic curve; DCA, decision curve analysis.

tors such as the grade of EPVS on the progression from MCI to AD, we first conducted a correlation analysis and univariate logistic regression analysis on the baseline data. Subsequently, we divided all data into a training set (85%, $n = 303$) and a validation set (15%, $n = 54$) for model building and internal validation. Variable selection was performed using the Least Absolute Shrinkage and Selection Operator (LASSO) regression model to enhance the accuracy of the predictive model. Non-zero variables from the LASSO regression results were included in single-factor and multiple-factor logistic regression

Table 1
Characteristics of patients in the MCI-C and MCI-NC group

Variable	MCI-C ($n = 176$)	MCI-NC ($n = 181$)	t/χ^2	p
Age (y)[a]	74.85 (6.88)	72.44 (8.00)	3.076	0.002
Sex (female) (%)	68 (38.6)	75 (41.4)	–0.539	0.590
APOE4 (%)			5.285	<0.001
0	57 (32.4)	107 (59.1)		
1	92 (52.3)	64 (35.4)		
2	27 (15.3)	10 (5.5)		
Hypertension (%)	77 (43.8)	81 (44.8)	–0.190	0.849
Diabetes (%)	15 (8.5)	16 (8.8)	–0.106	0.915
Hyperlipidemia (%)	22 (12.5)	32 (17.7)	–1.364	0.173
Hypercholesteremia (%)	15 (8.5)	25 (13.8)	–1.582	0.114
Aβ, pg/mL[a]	705.52 (338.84)	1094.40 (463.59)	–8.115	<0.001
Tau, pg/mL[a]	332.58 (123.10)	264.22 (116.11)	6.034	<0.001
p-tau, pg/mL[a]	32.39 (13.74)	24.60 (12.94)	6.449	<0.001
CDRSB, score[a]	1.85 (0.96)	1.25 (0.67)	6.409	<0.001
ADAS11, score[a]	13.16 (4.04)	7.99 (3.20)	11.214	<0.001
ADAS13, score[a]	21.32 (5.37)	13.03 (5.27)	11.857	<0.001
ADASQ4, score[a]	7.13 (1.95)	4.31 (2.23)	10.635	<0.001
MMSE, score[a]	26.61 (1.70)	28.18 (1.52)	–8.273	<0.001
CSOPVS (%)			9.190	<0.001
1	61 (34.7)	146 (80.7)		
2	57 (32.4)	28 (15.5)		
3	58 (33.0)	7 (3.9)		
BGPVS (%)			6.067	<0.001
1	113 (64.2)	165 (91.2)		
2	45 (25.6)	11 (6.1)		
3	18 (10.2)	5 (2.8)		
Ventricles, mm^3 [a]	47446.07 (23149.80)	37212.78 (21741.08)	4.857	<0.001
Hippocampus, mm^3 [a]	6047.02 (1020.37)	7127.90 (1066.04)	–9.058	<0.001
WholeBrain, mm^3 [a]	982892.59 (113286.19)	1065447.94 (110709.66)	–6.602	<0.001
Entorhinal, mm^3 [a]	3011.50 (719.00)	3735.17 (694.93)	–8.790	<0.001
Fusiform, mm^3 [a]	15793.77 (2432.75)	18419.69 (2547.35)	–8.824	<0.001
MidTemp, mm^3 [a]	17478.49 (2957.18)	20841.15 (2547.73)	–10.295	<0.001
ICV, mm^3 [a]	1572420.23 (173888.38)	1540804.31 (157733.55)	1.704	<0.001

AGE, Baseline age; *APOE4*, the numbers of Apolipoprotein ε4 allele; Hypertension, history of hypertension; Diabetes, history of diabetes; Hyperlipidemia, history of hyperlipidemia; Hypercholesteremia, history of hypercholesteremia; Aβ, amyloid-β 1–42 content in cerebrospinal fluid; Tau, tau protein content in cerebrospinal fluid; p-tau, phosphorylated tau protein content in cerebrospinal fluid; CDRSB, Clinical Dementia Rating Score; ADAS11, Alzheimer's disease assessment scale-cognitive score 11 items; ADAS13, Alzheimer's disease assessment scale-cognitive score 13 items; ADASQ4, Alzheimer's disease assessment scale-cognitive score delayed word recall; MMSE, Mini-Mental State Examination; CSOPVS, rating of centrum semiovale perivascular space; BGPVS, rating of basal ganglia perivascular space; Ventricles, ventricle volume; Hippocampus, hippocampus volume; WholeBrain, wholebrain volume; Entorhinal, entorhinal cortex volume; Fusiform, fusiform gyrus volume; MidTemp, middle temporal volume; ICV, intracranial volume. [a](mean (SD)).

for further screening and construction of a multivariate logistic regression model to predict the risk of MCI progression to AD, with the results visualised as a Nomogram.

Diagnostic accuracy, calibration performance, and net benefits served as the key assessment criteria in this study. These parameters were assessed through ROC curve analysis, calibration curve analysis, and decision curve analysis (DCA), respectively. The ROC curve can evaluate the model's discriminative ability. The closer the ROC curve is to the upper left corner, the larger the AUC value, indicating a better performance of the model in distinguishing between positive and negative cases. Generally, AUC ≥ 0.7 indicates satisfactory performance. Furthermore, using the calibration curve to assess the accuracy of the model's predicted probabilities, a closer match between the calibration curve and the actual probability curve indicates a better fit of the model in probability prediction. Lastly, decision curve analysis evaluates the utility of the model in different clinical scenarios by calculating the benefits and losses of patients at different thresholds, providing a comprehensive assessment of whether the model has practical clinical value.Furthermore, to evaluate the enhancement of models by EPVS levels,

we constructed multiple models and compared their performance using ROC curves and AUC values. Statistical analyses were executed using R software, with p-values below 0.05 deemed statistically significant.

RESULTS

Description of statistical results

Table 1 demonstrates the demographic characteristics and statistical results of the two groups of MCI-C and MCI-NC. The study encompassed 358 participants ranging in age from 65 to 80 years. The average age within the MCI-C group was 72.44 years (SD = 8), while the MCI-NC group had an average age of 74.85 years (SD = 6.88). As expected, the number and percentage of individuals with moderate (CSO-PVS = 2, 57 32.4%) and severe (CSO-PVS = 3, 58 33.0%) CSO-PVS grades were notably higher in the MCI-C group compared to the MCI-NC group with moderate (CSO-PVS = 2, 28 15.5%) and severe (CSO-PVS = 3, 7 3.9%) grades, and these findings were statistically significant ($p < 0.001$). Comparative analysis showed no significant differences in sex distribution or the prevalence of hypertension, diabetes, hyperlipidemia, or hypercholesterolemia between the MCI converters and non-converters in both cohorts ($p > 0.05$). The Mann-Whitney U test showed significantly higher counts of *APOE4* genotype, tau and p-tau levels in CSF, perivascular spaces grade in the centrum semiovale and basal ganglia, CDR-SB score, ADAS13, ADAS11, and ADASQ4 scores in the MCI-C group compared to the MCI-NC group ($p < 0.001$).Conversely, the MCI-C group showed significantly lower levels of Aβ in CSF, MMSE score, and volumes of the hippocampus, fusiform gyrus, entorhinal cortex, middle temporal, and wholebrain ($p < 0.001$).

Univariate logistic regression of baseline data

Univariate logistic regression analysis was conducted on variables with statistical significance ($p < 0.05$) from the baseline data to explore the association between PVS enlargement and the progression from MCI to AD. The results revealed a significant correlation between the degree of PVS enlargement in the centrum semiovale (CSO-PVS) and basal ganglia (BG-PVS) with the risk of disease advancement. Specifically, moderate enlargement of CSO-PVS (CSO-PVS = 2) displayed a substantial odds ratio (OR) of 5.54 (95% CI [3.04–10.18]), indicating a five-fold increase in the likelihood of progression. Furthermore, severe enlargement of CSO-PVS (CSO-PVS = 3) exhibited a notably high OR of 25.04 (95% CI [10.07–62.23]), emphasizing its strong predictive value for disease progression. Similarly, moderate enlargement of BG-PVS (BG-PVS = 2) demonstrated a significant OR of 9.26 (95% CI [3.97–21.6]), while severe enlargement of BG-PVS (BG-PVS = 3) had an OR of 4.98 (95% CI [1.75–14.20]), highlighting their predictive significance (Table 2).

Furthermore, age, *APOE4* genotype, CSF concentrations of Aβ, tau, and p-tau, scores from cognitive assessments including CDRSB, ADAS11, ADAS13, ADASQ4, MMSE, and volumetric measures of the hippocampus, fusiform gyrus, entorhinal cortex, and middle temporal gyrus all exhibited significant associations with the transition from MCI to AD. These variables served as independent predictors in the regression model. Nevertheless, the primary limitation of this approach is its inability to address potential interactions and collinearity among the variables.

Clinical feature selection

To construct and assess the accuracy of a predictive model for MCI-AD progression risk, 358 patients were randomly assigned to a training set ($n = 303$) and a validation set ($n = 54$), with an 85 : 15 split. 24 items clinical characteristics identified through univariate logistic regression were included in a subsequent LASSO regression analysis. This process identified 12 variables with non-zero coefficients (Fig. 2), encompassing the *APOE4* genotype, CSF Aβ content, CDRSB, ADAS11, ADASQ4, MMSE scale, and volumes of the fusiform gyrus (Fusiform), entorhinal cortex (Entorhinal), middle temporal (MidTemp) and intracranial volume (ICV) area, along with the perivascular space grade (CSO, BG). Incorporate these 12 variables into a multiple logistic regression, assessing their P-values, collinearity, and OR values to derive the final predictive model consisting of six variables: *APOE4* genotype, ADAS11 scale, CSO-PVS grade, and the volumes of Entorhinal, Fusiform, and MidTemp (Table 3).

Estimation of the predictive model

Utilizing stepwise logistic regression analysis, we identified *APOE4* genotype, ADAS11 scale, CSO-PVS grade, and the volumes of Entorhinal, Fusiform, and MidTemp as independent predictors for the con-

Table 2
Results of univariate logistic regression analysis of baseline data

Predictors	Univariate logistic regression analysis			
	β	OR	95% CI	*p*
AGE	0.0425	1.59	1.14–2.22	0.0065
APOE4 = 1	1.0612	2.89	1.76–4.75	<0.0001
APOE4 = 2	1.6843	5.39	2.31–12.57	<0.0001
Aβ	–0.0023	0.20	0.13–0.32	<0.0001
Tau	0.0049	1.96	1.47–2.61	<0.0001
p-tau	0.0444	2.00	1.48–2.70	<0.0001
CDRSB	0.91	2.48	1.81–3.40	<0.0001
ADAS11	0.4131	15.73	8.37–29.58	<0.0001
ADAS13	0.2910	18.36	9.56–35.25	<0.0001
ADASQ4	0.5844	7.73	4.77–12.53	<0.0001
MMSE	–0.6024	0.16	0.10–0.27	<0.0001
CSOPVS = 2	1.71	5.54	3.04–10.08	<0.001
CSOPVS = 3	3.22	25.04	10.07–62.23	<0.001
BGPVS = 2	2.2262	9.26	3.97–21.60	<0.001
BGPVS = 3	1.6072	4.98	1.75–14.20	0.0026
Ventricles	0.000019	1.77	1.31–2.42	0.0003
Hippocampus	–0.0009	0.23	0.15–0.34	<0.001
Entorhinal	–0.0015	0.18	0.12–0.29	<0.0001
Fusiform	–0.0004	0.20	0.13–0.31	<0.0001
MidTemp	–0.0004	0.16	0.10–0.25	<0.0001

OR, odds ratio; CI, confidence interval; *APOE4*, the numbers of Apolipoprotein ε4 allele; Aβ, amyloid-β 1–42 content in cerebrospinal fluid; Tau, tau protein content in cerebrospinal fluid; p-tau, phosphorylated tau protein content in cerebrospinal fluid; CDRSB, Clinical Dementia Rating Score; ADAS11, Alzheimer's disease assessment scale-cognitive score 11 items; ADAS13, Alzheimer's disease assessment scale-cognitive score 13 items; ADASQ4, Alzheimer's disease assessment scale-cognitive score delayed word recall; MMSE, Mini-Mental State Examination; CSOPVS, rating of centrum semiovale perivascular space; BGPVS, rating of basal ganglia perivascular space; Ventricles, ventricle volume; Hippocampus, hippocampus volume; Entorhinal, entorhinal cortex volume; Fusiform, fusiform gyrus volume; MidTemp, middle temporal volume.

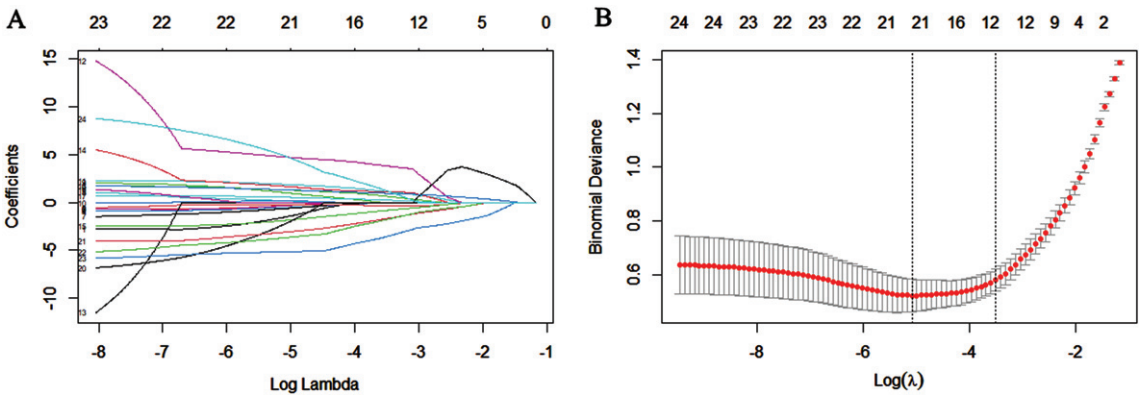

Fig. 2. Predictor selection was conducted using LASSO regression analysis with tenfold cross-validation. A coefficient profile plot was generated against the log (lambda) sequence to visualize the tuning parameter selection of deviance in the LASSO regression. In this study, predictor selection was based on the 1-SE criteria, resulting in the selection of 11 non-zero coefficients. LASSO stands for least absolute shrinkage and selection operator, and SE refers to standard error.

version of MCI to AD. The variance inflation factor (VIF) values of these predictors were all below 5, indicating the absence of significant collinearity among them (refer to Table 3). These six variables, including *APOE4* genotype, ADAS11 scale, CSOPVS grade, and the volumes of Entorhinal, Fusiform, and MidTemp, collectively formed the final predictive model. Subsequent validation of this model through ROC curve analysis revealed an impressive AUC of 0.956 (95% CI, 0.936–0.976) for the training dataset and 0.912 (95% CI, 0.839–0.985) for the validation set (see Fig. 3). To enhance the interpretability

Table 3
Final model for MCI-AD progression risk: Results of multivariate logistic regression variable analysis

Predictors	Final Model				
	β	OR	95% CI	*p*	VIF value
APOE4 = 1	0.92	2.51	1.08–5.84	0.0326	1.125
APOE4 = 2	1.99	7.30	1.81–29.47	0.0053	1.185
ADAS11	0.37	11.69	4.81–28.41	<0.0001	1.071
CSOPVS = 2	2.24	9.40	3.23–27.34	<0.0001	1.372
CSOPVS = 3	3.20	24.64	7.66–79.29	<0.0001	1.186
Entorhinal	–0.0007	0.43	0.21–0.86	0.0179	1.148
Fusiform	–0.0003	0.31	0.14–0.68	0.0035	1.564
MidTemp	–0.0003	0.34	0.17–0.66	0.0015	1.252

OR, odds ratio; CI, confidence interval; VIF, variance inflation factor; *APOE4*, the numbers of Apolipoprotein ε4 allele; ADAS11, Alzheimer's disease assessment scale-cognitive score 11 items; CSOPVS, rating of centrum semiovale perivascular space; Entorhinal, entorhinal cortex volume; Fusiform, fusiform gyrus volume; MidTemp, middle temporal volume.

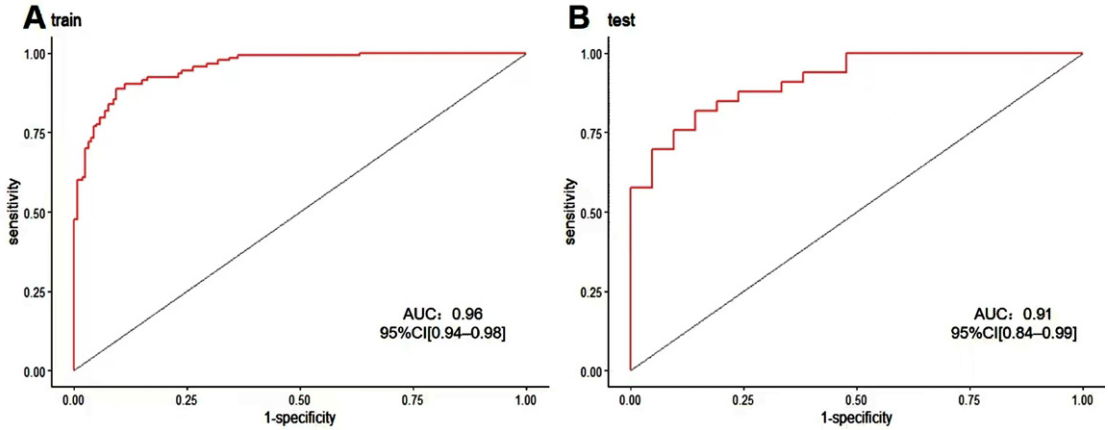

Fig. 3. The AUC represents the discriminatory ability of the model and was assessed for both the predictive model and internal validation. Panel A displays the AUC of the predictive model, while panel B exhibits the AUC of the internal validation using a validation set of $n = 54$. The dotted vertical lines indicate the 95% confidence interval. AUC stands for area under the curve.

of the predictive model, a nomogram was developed (depicted in Fig. 4), offering a practical clinical tool for estimating the probability of MCI patients progressing to AD.

Performance evaluation of the integrated model

In order to evaluate the significance of the CSO-PVS grade within predictive models and compare it with existing known biomarker models, we constructed a Basic model (excluding CSO-PVS while keeping other factors constant) for comparison, and subjected both models as well as single-factor components of the model to ROC curve analysis (Fig. 5). The results showed that in the training cohort, the model incorporating CSO-PVS (referred to as the PVS Model) exhibited the highest predictive accuracy of 0.96 (0.94–0.98), while the Basic model achieved 0.93 (0.90–0.95). This superior performance was also evident in the validation cohort with the PVS Model showing accuracy of 0.91 (0.84–0.99) compared to the Basic model's accuracy of 0.86 (0.77–0.96), indicating a significant improvement in model efficacy.The sensitivity (0.916) and specificity (0.80) of the PVS model are both superior to the base model. In the validation set, the sensitivity (0.848) and specificity (0.857) also indicate that the comprehensive predictive model with CSO-PVS has better discriminatory ability (Table 4). As a standalone biomarker, CSO-PVS also demonstrated good performance with an accuracy of 0.77 (0.72–0.82) in the validation set. Other independent risk factors including *APOE4*, ADAS11, Entorhinal cortex, Fusiform gyrus, and Middle Temporal volumes showed high accuracy, with corresponding values in the training cohort of 0.66 (0.60–0.71), 0.85 (0.81–0.89), 0.78 (0.73–0.83), 0.77 (0.72–0.82), and 0.82 (0.77–0.87), respectively. In the validation

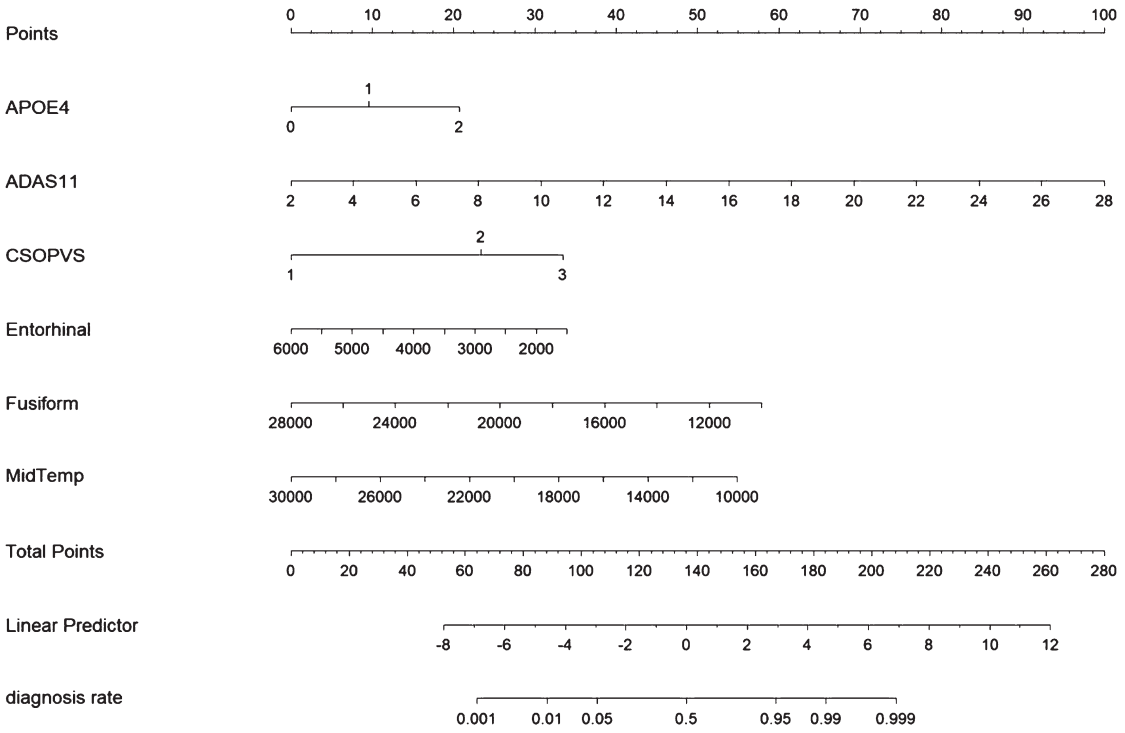

Fig. 4. The nomogram for predicting MCI-AD risk and its algorithm involves assigning points for each variable of an MCI patient on the uppermost rule. The scores are then summed to obtain the total number of points, and the corresponding predicted probability of progression to Alzheimer's disease is determined on the lowest rule.

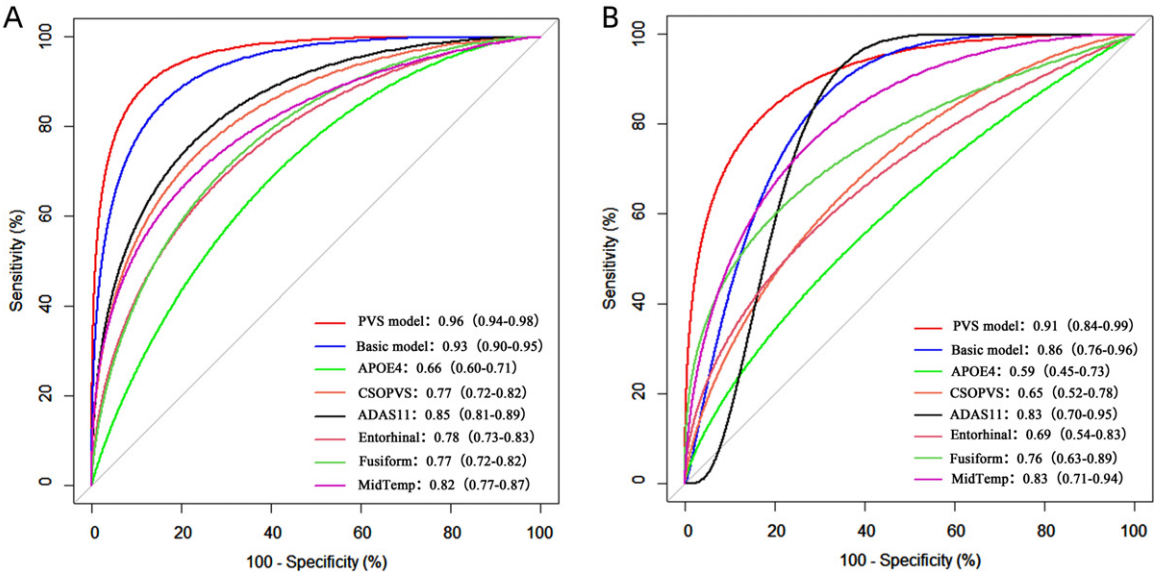

Fig. 5. ROC curves for the integrated model, Basic model and independent predictors in the model for the prediction of progression from MCI to AD in the training (a) and test (b) sets. PVS Model: Integrated predictive model (includes CSO-PVS grade). Basic Model: Comparative Model (excludes CSO-PVS grade while keeping the remaining factors unchanged). *APOE4*, the numbers of Apolipoprotein ε4; ADAS11, Alzheimer's disease assessment scale-cognitive score 11 items; CSOPVS, rating of centrum semiovale perivascular space; Entorhinal, entorhinal cortex volume; Fusiform, Fusiform gyrus volume; MidTemp, middle temporal volume.

Table 4
Comparison of predictive model performance

Predictors	Train			Test		
	AUC	Sensitivity	Specificity	AUC	Sensitivity	Specificity
PVS model	0.956	0.916	0.80	0.912	0.848	0.857
Basic model	0.926	0.860	0.769	0.862	0.788	0.809

PVS model, integrated model with CSO-PVS; Basic model, Remove only the base model of CSO-PVS; AUC, area under the curve.

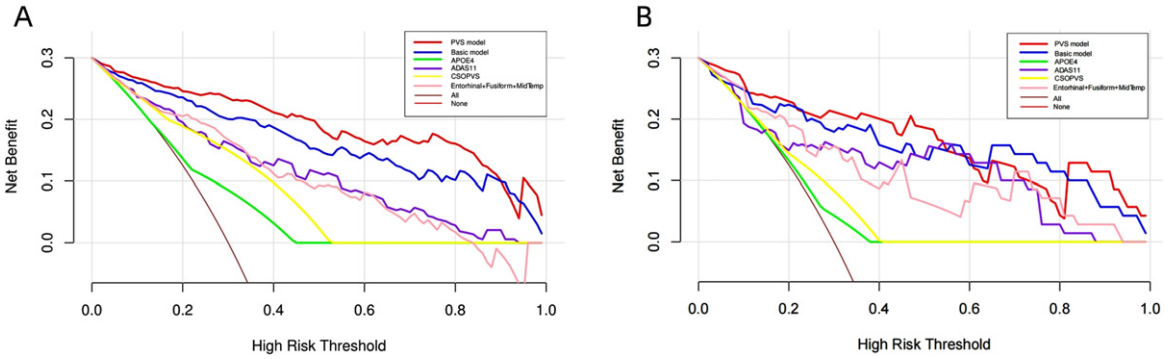

Fig. 6. DCA curves for the associativeintegrated model, Basic model and independent predictors in the model in the training (A) and test (B) sets. PVS Model: Integrated predictive model (includes CSO-PVS grade). Basic Model: Comparative Model (excludes CSO-PVS grade while keeping the remaining factors unchanged). *APOE4*, the numbers of Apolipoprotein $\varepsilon 4$; ADAS11, Alzheimer's disease assessment scale-cognitive score 11 items; CSOPVS, rating of centrum semiovale perivascular space; Entorhinal, entorhinal cortex volume; Fusiform, Fusiform gyrus volume; MidTemp, middle temporal volume.

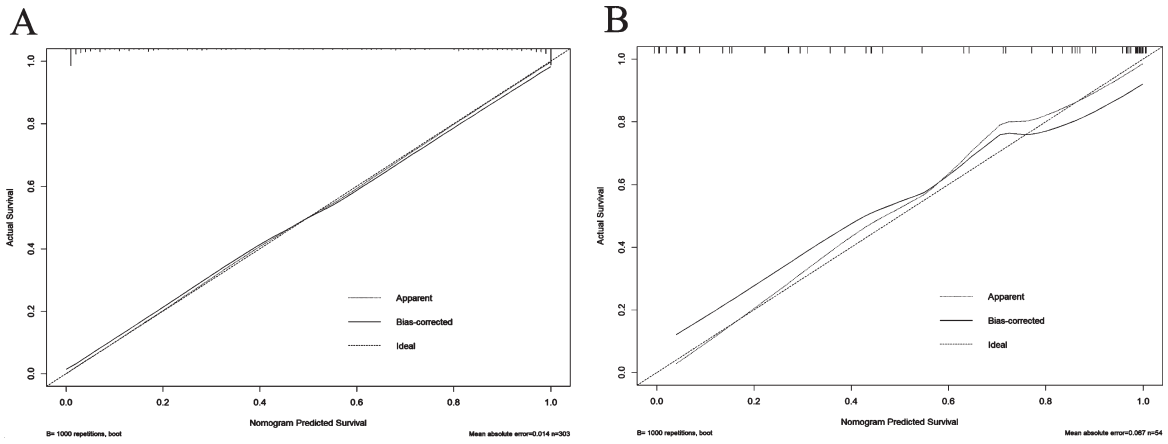

Fig. 7. A) Training set; B) Test set. The calibration curve of the predictive model illustrates the degree of consistency between the predicted probability and observed probability. The Hosmer–Lemeshow test, with a p-value greater than 0.05, suggests that the model exhibits goodness-of-fit.

cohort, the accuracies were 0.59 (0.45–0.73), 0.83 (0.70–0.95), 0.69 (0.54–0.83), 0.76 (0.63–0.89), and 0.83 (0.71–0.94) for *APOE4*, ADAS11, Entorhinal cortex, Fusiform gyrus, and Middle Temporal volumes, respectively. To further validate the model's value, we conducted DCA curve analysis on the PVS model, Basic model, *APOE4*, CSO-PVS grade, ADAS11 scale, and the integrated brain region volumes (Entorhinal+Fusiform+MidTemp) (Fig. 6). The DCA curve analysis revealed that the integrated predictive model incorporating CSO-PVS yielded the highest net benefit.The calibration curve (Fig. 7) demonstrates that the proposed model is well calibrated.

DISCUSSION

At present, no effective pharmacological interventions exist to arrest the progression of AD, emphasizing the importance of preventive measures and the postponement of its diagnosis and treatment. Therefore, the precise prediction of MCI patients' risk of developing AD, the identification of high-risk individuals, and the initiation of early interventions are challenging but essential goals. This research presents the perivascular space as a novel biomarker and constructs a predictive nomogram for assessing the risk of progression from MCI to AD. The nomogram aids clinicians in rapidly identifying patients at high risk, enabling early intervention and reducing the impact on patients and their families. The model incorporates seven variables: sex, *APOE* ε4 allele status, ADAS-Cog11 score, CSO-PVS grade, and volumes of the entorhinal cortex, fusiform gyrus, and mid-temporal region. It exhibits superior discriminative capacity, calibration, and clinical utility.

Prior research has demonstrated the significance of the perivascular space as a crucial pathway for metabolite elimination. Dysfunction in the brain's lymphatic system due to degeneration or natural aging leads to the accumulation of large molecules, such as Aβ, in the perivascular space, resulting in irreversible expansion that is observable through imaging.[9] Therefore, perivascular space expansion may serve as an imaging biomarker for the impairment of brain metabolism clearance pathways. Numerous studies have substantiated that enlargement of the perivascular spaces in the centrum semiovale can independently prognosticate dementia.[15,22] A study revealed that 40.9% of AD-related pathological participants had severe CSO-PVS, while the proportion for subcortical vascular cognitive impairment participants was 14.7%. In the same study, 0.91% of AD-related pathological participants exhibited severe BG-PVS, compared to 9.5% in subcortical vascular cognitive impairment participants.[23] Additionally, two studies based on 1.5T and 3.0T MRI results also indicated a higher level of EPVS grade (including CSO-PVS and BG-PVS) in the AD population.[24,25] In a longitudinal study based on the ADNI database, individuals with moderate and frequent/severe CSO-PVS had a higher risk of diagnostic conversion (including healthy-MCI, MCI-AD) compared to individuals with no/light CSO-PVS.[26] However, its efficacy as a biomarker for the risk of MCI advancing to AD remains to be fully ascertained. This research establishes a significant positive correlation between the severity of centrum semiovale perivascular spaces and the risk of MCI progressing to AD, suggesting that greater CSO-PVS severity augments the likelihood of progression.Within AD research, biomarkers are crucial for early diagnosis and prognosis, as evidenced by numerous studies and predictive models.[27] Among these, neuropsychological tests, biochemical assays, and neuroimaging are extensively examined for their diagnostic value.[28] Biochemical markers, however, are constrained by variability in testing methods and the invasive nature of certain procedures, such as CSF analysis. Neuropsychological evaluations are most informative with overt clinical symptoms due to their subjectivity. Among these approaches, neuroimaging has become paramount, with MRI providing a non-invasive insight into brain structures, thereby playing a vital role in AD research.[29–31] Consequently, the CSO-PVS severity observed in MRI scans may emerge as a key biomarker for transitioning from MCI to AD, supporting diagnostic and therapeutic strategies.

In this study, we performed a preliminary univariate logistic regression analysis on the degree of perivascular space enlargement to explore its potential as a predictive biomarker for the progression from MCI to AD across two patient cohorts.The findings indicate that both moderate (CSO-PVS = 2, OR = 5.54, 95% CI [3.04–10.18]) and severe (CSO-PVS = 3, OR = 25.04, 95% CI [10.07–62.23]) expansions of the perivascular spaces at the centrum semiovale are significant predictors of progression to AD, as reported in Table 2. These associations remained robust in the multivariate logistic regression model, which controlled for additional variables, demonstrating strong predictive capabilities (CSO-PVS = 2, OR = 9.40, 95% CI [3.23–27.34]; CSO-PVS = 3, OR = 24.64, 95% CI [7.66–79.29]), as shown in Table 3. It is important to note that some of the reported odds ratios are associated with wide confidence intervals (CI), reflecting the variability in the estimates due to the relatively small sample size in certain subcategories, particularly in severe enlargement groups. This limitation may have influenced the precision of the estimates and the width of the confidence intervals. Future studies with larger sample sizes in each subgroup are warranted to validate and strengthen the findings. Considering this limitation, even so, the results focusing on odds ratios (ORs) still demonstrate the significant predictive role of PVS enlargement in the transition from MCI to AD. Consequently, the enlargement of CSO-PVS may serve

as a significant prognostic indicator in the development of MCI into AD. However, the constraints of this study necessitate further corroboration through more extensive sampling and multicentric research. Moreover, while moderate (BG-PVS = 2, OR = 9.26, 95% CI [3.97–21.6]) and severe (BG-PVS = 3, OR = 4.98, 95% CI [1.75–14.20]) enlargements of perivascular spaces in the basal ganglia region exhibited predictive potential in univariate analyses, their prognostic relevance was not significant in the multivariate model that incorporated a range of variables. The predictive utility of basal ganglia PVS enlargement in the advancement of MCI to AD warrants additional exploration.

The univariate analysis of the variables examined in this study indicated no statistically significant differences ($p > 0.05$) between the groups in terms of sex, history of hypertension, diabetes, and hyperlipidemia. This finding is consistent with prior research on risk prediction models for the progression from MCI to AD.[7,8,32] In contrast, significant differences ($p < 0.05$) were noted in the age of participants, clinical cognitive function scores (ADAS-Cog13, CDR-SB, MMSE), presence of the *APOE* ε4 allele, CSF Aβ levels, CSF t-tau, and p-tau levels, as well as MRI-measured brain region volumes, including the hippocampus, entorhinal cortex, fusiform gyrus, middle temporal gyrus, and total brain volume. The severity of perivascular spaces in the centrum semiovale also differed between the MCI-AD conversion group and the non-conversion group. These outcomes corroborate findings from earlier studies.[33]

All patients were divided into a training group and a validation group to construct a predictive model. LASSO regression analysis was used to select appropriate clinical features, reduce collinearity, and improve model accuracy. This method is considered superior to univariate analysis in selecting predictive factors.[34,35] Subsequently, multivariate logistic regression analysis was performed on the 12 selected variables with non-zero coefficients. From this analysis, 6 clinical features with good predictive ability ($p < 0.05$) were identified and used to construct a predictive model, visualized as a nomogram. These 6 clinical features include *APOE4* genotype, ADAS11 scale, CSO-PVS grade, Entorhinal, Fusiform, and MidTemp volume. The predictive model, composed of these six clinical features, demonstrated excellent predictive ability in the validation of the ROC curve, with an AUC value of 0.912 (95% CI, 0.839–0.985). In comparison with the baseline model that excluded CSO-PVS grade and single factors in the model for ROC curve accuracy, models incorporating CSO-PVS demonstrated the highest accuracy. The baseline model had an AUC value of 0.86 (95% CI, 0.77–0.96) in the validation group. Further validation of the clinical applicability of the models using DCA curves showed that models including CSO-PVS exhibited the best clinical utility.

ApoE is the primary cholesterol carrier in the brain, contributing to neuronal growth, cell membrane repair and remodeling, Aβ clearance and degradation, and reduction of neuroinflammation.[36] The three alleles of *APOE—APOE2* (ε2/ε2, ε2/ε3), *APOE3* (ε3/ε3, ε2/ε4), and *APOE4* (ε3/ε4, ε4/ε4)—have been associated with varying AD risks. Studies have revealed that compared to patients carrying *APOE3* ε3/ε3, those carrying *APOE3* ε2/ε4 have a 1.64 times higher risk of developing AD, while those carrying *APOE4* ε3/ε4 have a 2.63 times higher risk, and those carrying *APOE4* ε4/ε4 have nearly a 14.00 times higher risk of developing AD.[37] *APOE4* is recognized as the most significant genetic risk factor for late-onset AD, implicated in the pathogenesis through the promotion of amyloid plaque and neurofibrillary tangle formation. Conversely, *APOE2* is associated with neuroprotective effects, potentially inhibiting or reversing these pathological processes.[38]

The ADAS-Cog with 11 items has demonstrated superior predictive validity for the progression from MCI to AD when assessing clinical cognitive function. This indicates that baseline impairments across multiple cognitive domains, as opposed to a singular evaluation of memory function, can more precisely forecast the risk of future dementia development.[39] Individuals with MCI exhibiting both memory and non-memory cognitive deficits are at increased risk for AD compared to those with memory deficits alone. Utilizing the ADAS-Cog to evaluate multiple cognitive domains enhances the accuracy of determining the MCI stage and improves prognostic accuracy.

Regarding MRI biomarkers, our model includes the severity of the centrum semiovale perivascular space and the volumes of the Entorhinal cortex, Fusiform gyrus, and Middle Temporal. Previous studies have demonstrated the diagnostic value and predictive performance of various potential MRI biomarkers, including whole brain atrophy, Middle Temporal, and Fusiform gyrus, in multiple machine learning studies for predicting MCI-AD risk.[40,41]

However, this prediction model has several limitations. First, its construction relies on the small sample

size of the ADNI database. Therefore, future studies should collect clinical and imaging data from a larger number of MCI patients. Second, this study only employs internal validation, and further verification through multi-center external validation is necessary to establish its clinical applicability. Lastly, the ADNI database used in this study lacks diversity in national ethnic origins, which hinders the determination of the model's universality in Asia and other regions.

Conclusion

We developed a nomogram in this study to predict the risk of progression to Alzheimer's disease in individuals with mild cognitive impairment by incorporating six imaging and clinical features, including perivascular space grades. This may facilitate clinicians in identifying high-risk patients with mild cognitive impairment more easily and quickly, enabling targeted treatment at an early stage to mitigate the impact of the disease.

AUTHOR CONTRIBUTIONS

Jun Chen (Conceptualization; Data curation; Formal analysis; Writing – original draft; Writing – review & editing); Jingwen Yang (Data curation; Formal analysis); Dayong Shen (Methodology; Software; Supervision); Xi Wang (Data curation); Zihao Lin (Data curation); Hao Chen (Conceptualization; Visualization; Writing – review & editing); Gui yun Cui (Validation; Visualization; Writing – review & editing); Zuohui Zhang (Conceptualization; Funding acquisition; Methodology; Writing – review & editing).

ACKNOWLEDGMENTS

Data collection and sharing for this project were funded by the ADNI (NIH grant U01 AG024904) and Department of Defense ADNI (Department of Defense award W81XWH12-2-0012). ADNI is funded by the National Institute on Aging, by the National Institute of Biomedical Imaging and Bioengineering, and through generous contributions from the following: AbbVie, Alzheimer's Association; Alzheimer's Drug Discovery Foundation; Araclon Biotech; BioClinica, Inc; Biogen; Bristol-Myers Squibb Co; CereSpir, Inc; Cogstate; Eisai Inc; Elan Pharmaceuticals, Inc; Eli Lilly and Com EuroImmun; F. Hoffmann-La Roche Ltd and its affiliated company Genentech, Inc; Fujirebio; GE Healthcare; IXICO Ltd; Janssen Alzheimer Immunotherapy Research & Development, LLC; Johnson & Johnson Pharmaceutical Research & Development LLC.; Lumosity; Lundbeck; Merck & Co, Inc; Meso Scale Diagnostics, LLC; NeuroRx Research; Neurotrack Technologies; Novartis Pharmaceuticals Corp; Pfifizer Inc; Piramal Imaging; Servier; Takeda Pharmaceutical Co; and Transition Therapeutics. The Canadian Institutes of Health Research is providing funds to support ADNI clinical sites in Canada. Private sector contributions are facilitated by the Foundation for the NIH (fnih.org). The grantee organization is the Northern California Institute for Research and Education, and the study is coordinated by the Alzheimer's Disease Cooperative Study at the University of California, San Diego. ADNI data are disseminated by the Laboratory for Neuro Imaging at the University of Southern California.

FUNDING

This work was supported by the Natural Science Foundation of Jiangsu Province (grant no. BK20150219).

CONFLICT OF INTEREST

The authors have no conflict of interest to report.

DATA AVAILABILITY

The data supporting the findings of this study are available on request from the corresponding author.

REFERENCES

1. 2022 Alzheimer's disease facts and figures. *Alzheimers Dement* 2022; 18: 700–789.
2. Global Action Plan on the Public Health Response to Dementia 2017–2025. Geneva: World Health Organization, 2017.
3. Petersen RC. Mild cognitive impairment. *Lancet* 2006; 367: 1979.
4. Da X, Toledo JB, Zee J, et al. Integration and relative value of biomarkers for prediction of MCI to AD progression: spatial patterns of brain atrophy, cognitive scores, APOE genotype and CSF biomarkers. *Neuroimage Clin* 2013; 4: 164–173.

5. Dickerson BC, Wolk DA; Alzheimer's Disease Neuroimaging Initiative. Biomarker-based prediction of progression in MCI: Comparison of AD-signature and hippocampal volume with spinal fluid amyloid-β and tau. *Front Aging Neurosci* 2013; 5: 55.
6. Salvatore C, Cerasa A and Castiglioni I. MRI characterizes the progressive course of ad and predicts conversion to Alzheimer's dementia 24 months before probable diagnosis. *Front Aging Neurosci* 2018; 10: 135.
7. Shu ZY, Mao DW, Xu YY, et al. Prediction of the progression from mild cognitive impairment to Alzheimer's disease using a radiomics-integrated model. *Ther Adv Neurol Disord* 2021; 14: 17562864211029551.
8. Jang H, Park J, Woo S, et al. Prediction of fast decline in amyloid positive mild cognitive impairment patients using multimodal biomarkers. *Neuroimage Clin* 2019; 24: 101941.
9. Iliff JJ, Wang M, Liao Y, et al. A paravascular pathway facilitates CSF flow through the brain parenchyma and the clearance of interstitial solutes, including amyloid β. *Sci Transl Med* 2012; 4: 147ra111.
10. Wardlaw JM, Benveniste H, Nedergaard M, et al. Perivascular spaces in the brain: anatomy, physiology and pathology. *Nat Rev Neurol* 2020; 16: 137–153.
11. Wilcock DM, Vitek MP and Colton CA. Vascular amyloid alters astrocytic water and potassium channels in mouse models and humans with Alzheimer's disease. *Neuroscience* 2009; 159: 1055–1069.
12. Wardlaw JM, Smith EE, Biessels GJ, et al. Neuroimaging standards for research into small vessel disease and its contribution to ageing and neurodegeneration. *Lancet Neurol* 2013; 12: 822–838.
13. Francis F, Ballerini L and Wardlaw JM. Perivascular spaces and their associations with risk factors, clinical disorders and neuroimaging features: A systematic review and meta-analysis. *Int J Stroke* 2019; 14: 359–371.
14. Ding J, Sigurdsson S, Jónsson PV, et al. Large perivascular spaces visible on magnetic resonance imaging, cerebral small vessel disease progression, and risk of dementia: The Age, Gene/Environment Susceptibility-Reykjavik Study. *JAMA Neurol* 2017; 74: 1105–1112.
15. Smeijer D, Ikram MK and Hilal S. Enlarged perivascular spaces and dementia: a systematic review. *J Alzheimers Dis* 2019; 72: 247–256.
16. Hansson O, Seibyl J, Stomrud E, et al. CSF biomarkers of Alzheimer's disease concord with amyloid-β PET and predict clinical progression: A study of fully automated immunoassays in BioFINDER and ADNI cohorts. *Alzheimers Dement* 2018; 14: 1470–1481.
17. Saykin AJ, Shen L, Yao X, et al. Genetic studies of quantitative MCI and AD phenotypes in ADNI: Progress, opportunities, and plans. *Alzheimers Dement* 2015; 11: 792–814.
18. Hsu YY, Schuff N, Du AT, et al. Comparison of automated and manual MRI volumetry of hippocampus in normal aging and dementia. *J Magn Reson Imaging* 2002; 16: 305–310.
19. Landau SM, Harvey D, Madison CM, et al. Associations between cognitive, functional, and FDG-PET measures of decline in AD and MCI. *Neurobiol Aging* 2011; 32: 1207–1218.
20. Weiner MW and Veitch DP. Introduction to special issue: Overview of Alzheimer's Disease Neuroimaging Initiative. *Alzheimers Dement* 2015; 11: 730–733.
21. Doubal FN, Maclullich AMJ, Ferguson KJ, et al. Enlarged perivascular spaces on MRI are a feature of cerebral small vessel disease. *Stroke* 2010; 41: 450–454.
22. Ding J, Sigurdsson S, Jónsson PV, et al. Large perivascular spaces visible on magnetic resonance imaging, cerebral small vessel disease progression, and risk of dementia. JAMA Neurol 2017; 74: 1105–1112.
23. Gargi B, Jin KH, Zoe F, et al. MRI-visible perivascular space location is associated with Alzheimer's disease independently of amyloid burden. *Brain* 2017; 140: 1107–1116.
24. Hansen TP, Cain J, Thomas O, et al. Dilated perivascular spaces in the Basal Ganglia are a biomarker of small-vessel disease in a very elderly population with dementia. *AJNR Am J Neuroradiol* 2015; 36: 893–898.
25. Martinez-Ramirez S, Pontes-Neto OM, Dumas AP, et al. Topography of dilated perivascular spaces in subjects from a memory clinic cohort. *Neurology* 2013; 80: 1551–1556.
26. Wang ML, Zou QQ, Sun Z, et al. Associations of MRI-visible perivascular spaces with longitudinal cognitive decline across the Alzheimer's disease spectrum. *Alzheimers Res Ther* 2022; 14: 185.
27. Veitch DP, Weiner MW, Aisen PS, et al. Understanding disease progression and improving Alzheimer's disease clinical trials: Recent highlights from the Alzheimer's Disease Neuroimaging Initiative. *Alzheimers Dement* 2019; 15: 106–152.
28. Tan CC, Yu JT and Tan L. Biomarkers for preclinical Alzheimer's disease. *J Alzheimers Dis* 2014; 42: 1051–1069.
29. Márquez F and Yassa MA. Neuroimaging biomarkers for Alzheimer's disease. *Mol Neurodegener* 2019; 14: 21.
30. Bozzali M, Serra L and Cercignani M. Quantitative MRI to understand Alzheimer's disease pathophysiology. *Curr Opin Neurol* 2016; 29: 437.
31. Chandra A, Dervenoulas G, Politis M, et al. Magnetic resonance imaging in Alzheimer's disease and mild cognitive impairment. *J Neurol* 2019; 266: 1293–1302.
32. Tang L, Wu X, Liu H, et al. Individualized prediction of early Alzheimer's disease based on magnetic resonance imaging radiomics, clinical, and laboratory examinations: a 60-month follow-up study. *J Magn Reson Imaging* 2021; 54: 1647–1657.
33. Chen Y, Qian X and Zhang Y, et al. Prediction models for conversion from mild cognitive impairment to Alzheimer's disease: a systematic review and meta-analysis. *Front Aging Neurosci* 2022; 14: 840386.
34. Tibshirani R. The lasso method for variable selection in the Cox model. *Stat Med* 1997; 16: 385–395.
35. Balachandran VP, Gonen M, Smith JJ, et al. Nomograms in oncology: more than meets the eye. *Lancet Oncol* 2015; 16: e173–e180.
36. Liu CC, Liu CC, Kanekiyo T, et al. Apolipoprotein E and Alzheimer disease: risk, mechanisms and therapy. *Nat Rev Neurol* 2013; 9: 106–118.
37. Yamazaki Y, Zhao N, Caulfield TR, et al. Apolipoprotein E and Alzheimer disease: pathobiology and targeting strategies. *Nat Rev Neurol* 2019; 15: 501–518.
38. Lanfranco MF, Ng CA and Rebeck GW. ApoE lipidation as a therapeutic target in Alzheimer's disease. *Int J Mol Sci* 2020; 21: 6336.
39. Korolev IO, Symonds LL and Bozoki AC. Predicting progression from mild cognitive impairment to Alzheimer's dementia using clinical, MRI, and plasma biomarkers via

probabilistic pattern classification. *PLoS One* 2016; 11: e138866.

40. Frisoni GB, Fox NC, Jack CJ, et al. The clinical use of structural MRI in Alzheimer disease. *Nat Rev Neurol* 2010; 6: 67–77.
41. Gómez-Sancho M, Tohka J and Gómez-Verdejo V. Comparison of feature representations in MRI-based MCI-to-AD conversion prediction. *Magn Reson Imaging* 2018; 50: 84–95.